Electronic Structure of Metallocenes

Y. S. Sohn, David N. Hendrickson, and Harry B. Gray*

Contribution No. 4104 from the Arthur Amos Noyes Laboratory of Chemical Physics, California Institute of Technology, Pasadena, California 91109.
Received July 20, 1970

Abstract: The electronic absorption spectra of various low-spin d^5 and d^6 metallocene complexes have been studied in different environments (glasses, KBr pellets, and single crystals) and as a function of temperature. Ferrocene, phenylferrocene, ruthenocene, and cobalticenium ion were selected in the d^6 study and several ferricenium, *n*-butylferricenium, and 1,1′-di-*n*-butylferricenium salts were examined in the d^5 case. The electronic spectra of ferrocene and phenylferrocene single crystals at 4.2°K clearly indicate that the bands at 22,700 and 22,400 cm^{-1}, respectively, consist of two electronic transitions each. The corresponding band systems in ruthenocene and cobalticenium ion also exhibit asymmetry at 77°K. Ligand-field theory has been successfully applied to the above d^6 metallocenes, utilizing the three observed spin-allowed d–d absorption band positions. The visible absorption spectra of the various ferricenium complexes show a low-energy charge-transfer transition (16,200 cm^{-1} in the unsubstituted ion). Ring substitution and temperature effects have been used to assign this band to the ligand-to-metal $^2E_{2g} \rightarrow {}^2E_{1u}$ transition. The vibrational structure observed for this band at 77°K appears as a doubled progression of the lowest energy a_{1g} vibration. The doubling has been attributed to splitting of the $^2E_{1u}$ excited state. Detailed assignments of this vibrational structure are given for $[Fe(cp)_2]PF_6$ and $[Fe(cp)_2](CCl_3CO_2H)_3$. The intense charge-transfer band of ferrocene ($\sim$50,000 cm^{-1}) as well as the corresponding bands in the other d^6 metallocenes have been assigned as ligand-to-metal transitions. A similar assignment has been proposed for the three strong ($f \approx 0.1$) bands observed in the ferricenium ultraviolet absorption spectrum.

Since its discovery in 1951,[1,2] ferrocene has played an important role, both theoretically and experimentally, in developing an understanding of the electronic structures of organometallic compounds. On the theoretical side the studies have included numerous MO calculations[3–12] as well as some qualitative crystal-field approaches.[13–16] From the reviews of these works by Rosenblum,[17] Brown,[18] and Ballhausen and Gray,[19] it is evident that none of the calculations is successful in explaining the totality of experimental facts.

The theoretical studies do give, however, a useful qualitative framework for the interpretation of various physical properties. For instance, the MO calculations in general indicate that the highest occupied orbitals are a_{1g} and e_{2g}, with the lowest unoccupied level being e_{1g}. Esr and magnetic susceptibility studies on the ferricenium ion,[20,21] its carborane analogs,[22] vanadocene, and nickelocene[23] are in agreement with a level ordering of $e_{2g} \sim a_{1g} < e_{1g}$.

The most powerful tool for locating the excited states and checking various features of the bonding theories of ferrocene is optical spectroscopy. Consequently, the ferrocene ultraviolet and visible spectra have been extensively studied by Scott and Becker,[24] and more recently by Armstrong, *et al.*,[25] Smith and Meyer,[26] and Stephenson and Winterrowd.[27] Very recently we communicated[28] the results of a 4.2°K visible absorption spectroscopic study of ferrocene and proposed assignments for the three spin-allowed d–d transitions. Improved resolution of the lowest energy (4400 Å) ferrocene band provided the key to this assignment scheme.

In this paper the results of a detailed absorption spectral study of several d^5 and d^6 metallocenes are given. In the case of the d^6 metallocenes, ferrocene will be used as a model compound. The resolution into two bands of the lowest energy visible peak observed for ferrocene[28] will be shown to be general. We have analyzed these two bands and a slightly higher energy band (3250 Å in ferrocene) as d–d transitions and obtained ligand-field parameters which are used to predict the positions of the spin-forbidden d–d bands.

In another recent communication[21] the lowest energy electronic band in the ferricenium ion was shown to be a $^2E_{2g} \rightarrow {}^2E_{1u}$ transition, in disagreement with previous reports.[29,30] Low-temperature spectral data for various

(1) T. J. Kealy and P. L. Pauson, *Nature (London)*, **168**, 1039 (1951).
(2) S. A. Miller, J. A. Tebboth, and J. F. Tremaine, *J. Chem. Soc.*, 632 (1952).
(3) H. H. Jaffe, *J. Chem. Phys.*, **21**, 156 (1953).
(4) J. D. Dunitz and L. E. Orgel, *ibid.*, **23**, 954 (1955).
(5) W. Moffit, *J. Amer. Chem. Soc.*, **76**, 3386 (1954).
(6) M. Yamazaki, *J. Chem. Phys.*, 24, 1260 (1956).
(7) E. Ruch, *Recl. Trav. Chem. Pays-Bas*, **75**, 638 (1956).
(8) E. M. Shustorovich and M. E. Dyatkina, *Dokl. Akad. Nauk SSSR*, **128**, 1234 (1959); **131**, 113 (1960); **133**, 141 (1960).
(9) J. P. Dahl and C. J. Ballhausen, *Kgl. Dan. Vidensk. Selsk., Mat.-Fys. Medd.*, **33** (5) (1961).
(10) R. D. Fischer, *Theor. Chim. Acta*, **1**, 418 (1963).
(11) A. T. Armstrong, D. G. Carroll, and S. P. McGlynn, *J. Chem. Phys.*, **47**, 1104 (1967).
(12) J. H. Schachtschneider, R. Prins, and P. Ros, *Inorg. Chim. Acta*, **1**, 462 (1967).
(13) A. D. Liehr and C. J. Ballhausen, *Acta Chem. Scand.*, **11**, 207 (1957).
(14) F. A. Matsen, *J. Amer. Chem. Soc.*, **81**, 2023 (1959).
(15) R. E. Robertsen and H. M. McConnell, *J. Phys. Chem.*, **64**, 70 (1960).
(16) D. R. Scott and R. S. Becker, *J. Organometal. Chem.*, 4, 409 (1965).
(17) M. Rosenblum, "Chemistry of the Iron Group Metallocenes," Wiley-Interscience, New York, N. Y., 1965.
(18) D. A. Brown, *Transition Metal Chem.*, **3**, 36 (1966).
(19) C. J. Ballhausen and H. B. Gray in "Chemistry of the Coordination Compounds," Vol. I, A. E. Martell, Ed., Van Nostrand-Reinhold, 1971, Chapter 1.
(20) R. Prins and F. J. Reinders, *J. Amer. Chem. Soc.*, **91**, 4929 (1969).
(21) Y. S. Sohn, D. N. Hendrickson, and H. B. Gray, *ibid.*, **92**, 3233 (1970).
(22) A. H. Maki and T. E. Berry, *ibid.*, **87**, 4437 (1965).
(23) R. Prins and J. D. W. van Voorst, *J. Chem. Phys.*, **49**, 4465 (1968).
(24) D. R. Scott and R. S. Becker, *ibid.*, **35**, 516 (1961).
(25) A. T. Armstrong, D. G. Carroll, and S. P. McGlynn, *ibid.*, **46**, 4321 (1967).
(26) J. J. Smith and B. Meyer, *ibid.*, **48**, 5436 (1968).
(27) P. B. Stephenson and W. E. Winterrowd, *ibid.*, **52**, 3308 (1970).
(28) Y. S. Sohn, D. N. Hendrickson, J. H. Smith, and H. B. Gray, *Chem. Phys. Lett.*, **6**, 499 (1970).
(29) D. A. Levy and L. E. Orgel, *Mol. Phys.* 4, 93 (1961).
(30) D. R. Scott and R. S. Becker, *J. Phys. Chem.*, **69**, 3207 (1965).

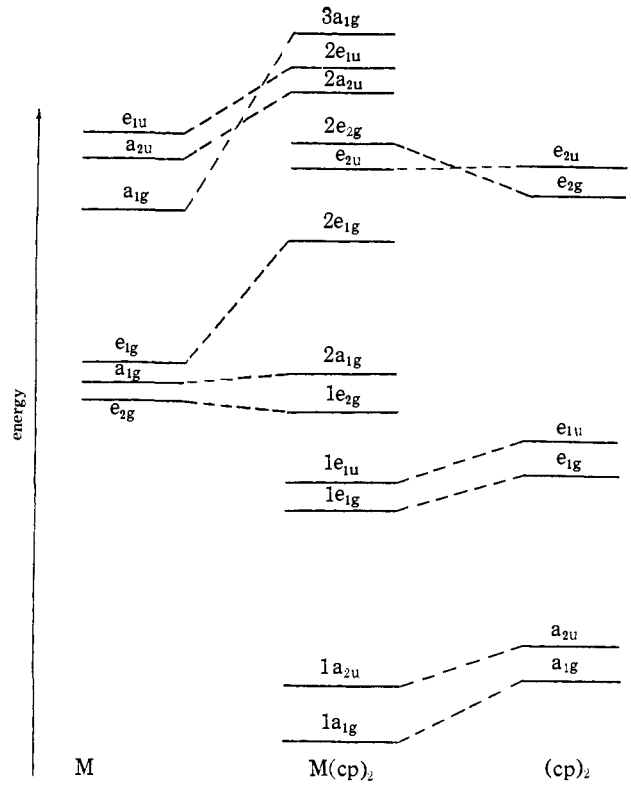

Figure 1. Estimated relative e^{core} energies for the molecular orbitals in metallocene complexes.

ferricenium salts, unsubstituted as well as substituted, are shown to support the $^2E_{2g} \rightarrow {}^2E_{1u}$ assignment, and a detailed interpretation of the observed vibrational structure is given. A ligand-field treatment of the d–d transitions for the ferricenium ion also is developed and compared with experimental results. Finally, the ultraviolet bands of both d^6 and d^5 metallocene complexes have been assigned.

Experimental Section

Preparation and Purification of Compounds. Ferrocene from two different sources (Alfa and Eastman Kodak) was used after purification. No spectral difference was noted between the purified materials. Purification was carried out by recrystallization in ethanol, followed by repeated sublimation *in vacuo* and finally zone refining. Transparent single-crystal plates of ferrocene were grown in reagent grade absolute ethanol by slow evaporation.

Ruthenocene, $Ru(C_5H_5)_2$ (Research Inorganics), was recrystallized in ethanol and sublimed twice *in vacuo*. Light yellow single crystals with well-developed faces were obtained.

$[Co(C_5H_5)_2]ClO_4$. To an aqueous solution of cobalticenium picrate[31] was added a slight excess of perchloric acid and the resultant picric acid was extracted with ether. The perchlorate solution was concentrated and cooled in ice. Light orange needles were obtained. *Anal.* (Galbraith) Calcd for $[Co(C_5H_5)_2]ClO_4$: Co, 20.42; C, 41.62; H, 3.49; Cl, 12.28. Found: Co, 20.25; C, 41.83; H, 3.62; Cl, 12.21.

$Fe(C_6H_5\text{-}C_5H_4)(C_5H_5)$. Phenylation of ferrocene was accomplished by the method of Broadhead and Pauson.[32] Monophenylferrocene was isolated using an alumina column; reddish orange needles (mp 111°, lit.[33] 109–110°) were obtained by repeated recrystallization in acetone. Further identification was obtained by a nmr spectrum. Transparent single-crystal plates of phenylferrocene were grown in reagent grade acetone by slow evaporation.

$[Fe(C_5H_5)_2](CCl_3CO_2H)_3$.[34] Ferrocene (10 mmol) and trichloroacetic acid (60 mmol) were allowed to react in 30 ml of benzene at room temperature for a day. The benzene was then slowly evaporated, giving crystals of the desired compound (mp 129–130°; lit.[34] 126–128°). *Anal.* Calcd for $[Fe(C_5H_5)_2](CCl_3CO_2H)_3$: Fe, 8.26; Cl, 47.19; C, 28.42; H, 1.94. Found: Fe, 8.54; Cl, 47.44; C, 28.55; H, 2.11.

$[Fe(C_5H_5)_2]BF_4$, $[Fe(C_5H_5)_2]PF_6$, $[Fe(n\text{-}C_4H_9\text{-}C_5H_4)(C_5H_5)]PF_6$, and $[Fe(n\text{-}C_4H_9\text{-}C_5H_4)_2]PF_6$ were prepared as reported previously.[35]

Solvents and Liquid Glasses. The following solvents for room-temperature spectral measurements or for low-temperature glass preparation were used without further purification: spectroquality acetonitrile, methanol, and EPA (ethyl ether, isopentane, and ethanol in volume ratio of 5:5:2), and anhydrous USP-NF grade ethanol.

Propionitrile (Eastman Kodak) was further purified by repeated fractional distillation. Chromatoquality (MC&B) 2-methyltetrahydrofuran (2-MTHF) was distilled from $LiAlH_4$ to remove peroxides and residual water.

When EPA was not a suitable solvent the following solvent mixtures were used for low-temperature glasses: 2-Me-THF and ethanol (1:2); ethyl ether, propionitrile, and ethanol (3:1:1); ethanol and methanol (5:1); and 10 *M* aqueous LiCl solution. Ir spectrograde KBr powder (MC&B) was used in the preparation of KBr pellets.

Absorption Spectral Measurements. Visible and near-ultraviolet absorption spectra were usually recorded on a Cary Model 14 CMRI spectrophotometer equipped with both a Cary low-temperature dewar modified to hold a standard 1.00-cm cell and with another quartz dewar designed for direct immersion of the sample cell into the liquid nitrogen. With this latter dewar a sample can be cooled down to liquid nitrogen temperature in a few minutes.

The following procedure was used in obtaining the relative-intensity spectra of various species (using the Cary spectrophotometer) at room and liquid nitrogen temperatures. Solutions of $Fe(C_5H_5)_2$, $Ru(C_5H_5)_2$, $Fe(C_6H_5\text{-}C_5H_4)(C_5H_5)$, and $[Co(C_5H_5)_2]ClO_4$ were prepared by dissolution in an appropriate organic solvent mixture. The room-temperature spectrum was recorded with the solution in the dewar and then liquid nitrogen was added for the low-temperature (77°K) measurement. This procedure gave relative intensity measurements after correction for solvent contraction at the lower temperature. Bubbling of the liquid nitrogen was prevented by cooling under reduced pressure. Window fogging was eliminated by continuous flushing of the sample compartment with dry nitrogen gas. Room-temperature and 77°K absorption spectra for various ferricenium compounds in KBr pellets were also obtained using the above technique employing the quartz dewar in the Cary instrument. The ferricenium ion is very unstable in most organic solvents, even acetonitrile and nitromethane. It is well known, however, that the ferricenium ion is fairly stable in acidic aqueous solution. We carefully checked spectroscopically the stability of various ferricenium salts in the neutral LiCl solution used for the low-temperature glass and no evidence for decomposition was detected for at least 1 hr.

Exact solution absorption band intensity measurements at room temperature were completed on the Cary instrument (without dewar) using the following solvents: ethanol, isopentane, and EPA for ferrocene, ruthenocene, and phenylferrocene; acetonitrile and water for $[Co(C_5H_5)_2]ClO_4$; 0.01 *M* $HClO_4$ solution for the ferricenium salts.

The single-crystal visible spectra of ferrocene and phenylferrocene were measured photographically on a Jarrell-Ash 0.75-m instrument equipped with a grating blazed at 10,000 Å. Well-formed crystals of ferrocene and phenylferrocene were mounted between two quartz plates and lowered slowly into liquid nitrogen. After a short annealing period, the crystals were cooled rapidly in liquid helium. Approximately one-half of the crystals powdered during such treatment, in agreement with previous observations.[27] Band II of ferrocene and phenylferrocene was recorded in second order using a tungsten lamp source, Kodak 103a-F plates, and Corning filters 3-74 and 4-97, which pass light between 3800 and 6000 Å. Band III of ferrocene was recorded in third order using a 150-W xenon lamp source, Kodak 103a-O plates, a water filter, and a Corning filter 7-54 which passes only ultraviolet light below 3900 Å.

Theory

In the solid state the molecular symmetry of ferrocene is D_{5d}. The cyclopentadienyl π basis orbitals can be

(31) G. Wilkinson, *J. Amer. Chem. Soc.*, 74, 6148 (1952).
(32) G. D. Broadhead and P. L. Pauson, *J. Chem. Soc.*, 367 (1955).
(33) M. Rosenblum, *J. Amer. Chem. Soc.*, **81**, 4530 (1959).
(34) M. Aly, R. Bramley, J. Upadhyay, A. Wasserman, and P. Woolliams, *Chem. Commun.*, 404 (1965).
(35) D. N. Hendrickson, Y. S. Sohn, and H. B. Gray, *Inorg. Chem.*, in press.

Table I.[a] Ligand-Field Transitions of d^6 and d^5 Metallocenes

	Transitions	Transition-energy expressions[b]
d^6	$^1A_{1g} \rightarrow a^1E_{1g}$	$\epsilon^c(e_{1g}) - \frac{1}{2}[\epsilon^c(e_{2g}) + \epsilon^c(a_{1g})] + 6B - C - \frac{1}{2}X$
	$\rightarrow b^1E_{1g}$	$\epsilon^c(e_{1g}) - \frac{1}{2}[\epsilon^c(e_{2g}) + \epsilon^c(1_{1g})] + 6B - C + \frac{1}{2}X$
	$\rightarrow {}^1E_{2g}$	$\epsilon^c(e_{1g}) - \epsilon^c(e_{2g}) - 9B - C$
	$^1A_{1g} \rightarrow a^3E_{1g}$	$\epsilon^c(e_{1g}) - \frac{1}{2}[\epsilon^c(e_{2g}) + \epsilon^c(a_{1g})] - B - 3C - \frac{1}{2}Y$
	$\rightarrow b^3E_{1g}$	$\epsilon^c(e_{1g}) - \frac{1}{2}[\epsilon^c(e_{2g}) + \epsilon^c(a_{1g})] - B - 3C + \frac{1}{2}Y$
	$\rightarrow {}^3E_{2g}$	$\epsilon^c(e_{1g}) - \epsilon^c(e_{2g}) - 9B - 3C$
d^5	$^2E_{2g} \rightarrow a^2A_{1g}$	$\epsilon^c(e_{2g}) - \epsilon^c(a_{1g}) + 20B$
	$\rightarrow b^2A_{1g}$	$\epsilon^c(e_{1g}) - \epsilon^c(e_{2g}) - 3B - C$
	$\rightarrow {}^2A_{2g}$	$\epsilon^c(e_{1g}) - \epsilon^c(e_{2g}) - 3B - C$
	$\rightarrow a^2E_{2g}$	$\epsilon^c(e_{1g}) - \frac{1}{2}[\epsilon^c(e_{2g}) + \epsilon^c(a_{1g})] + 5B - C - \frac{1}{2}Z$
	$\rightarrow b^2E_{2g}$	$\epsilon^c(e_{1g}) - \frac{1}{2}[\epsilon^c(e_{2g}) + \epsilon^c(a_{1g})] + 5B - C + \frac{1}{2}Z$
	$\rightarrow a,b,c^2E_{1g}$	$\epsilon^c(e_{1g}) - \epsilon^c(a_{1g}) + 7B - C^c$
		$\epsilon^c(e_{1g}) - \epsilon^c(e_{2g}) + 3B - 2C^c$
		$\epsilon^c(e_{1g}) - \epsilon^c(e_{2g}) - 3B - 3C^c$

[a] Here the ϵ^c's are one-electron core energies and B and C are Racah electron repulsion parameters. [b] $X = \{[\epsilon^c(e_{2g}) - \epsilon^c(a_{1g}) + 6B]^2 + 384B^2\}^{1/2}$, $Y = \{[\epsilon^c(e_{2g}) - \epsilon^c(a_{1g}) + 16B]^2 + 96B^2\}^{1/2}$, $Z = \{[\epsilon^c(e_{2g}) - \epsilon^c(a_{1g}) + 4B]^2 + 192B^2\}^{1/2}$. [c] These expressions as given do not include configurational interactions; see Theory section.

classified in this symmetry and ordered in energy as shown in Figure 1. The iron valence orbitals (see Figure 1) transform as $a_{1g}(3d)$, $e_{1g}(3d)$, $e_{2g}(3d)$, $a_{1g}(4s)$, $a_{2u}(4p)$, and $e_{1u}(4p)$.

A useful molecular orbital energy level diagram for ferrocene may be constructed from the above symmetry considerations and from the values of overlap integrals between the ring and the metal orbitals. The best available iron and carbon π orbitals give[9]

$S(a_{1g})_d$	$S(e_{1g})$	$S(e_{2g})$	$S(a_{1g})_s$	$S(a_{2u})$	$S(e_{1u})$
0.030	0.148	0.079	0.527	0.236	0.468

Strong bonds between the metal orbitals $a_{1g}(4s)$, $a_{2u}(4p)$, and $e_{1u}(4p)$ and the carbon π orbitals result in placing their corresponding antibonding levels high in energy. Of the 3d orbitals of the metal, the e_{1g} set has the greatest overlap with the ring orbitals and thus should form relatively strong bonds. These considerations were put forward in a recent review[19] as the basis of the estimated energy level diagram for ferrocene which is reproduced in Figure 1. The ground state of d^6 ferrocene is $^1A_{1g}$-$(1e_{2g})^4(2a_{1g})^2$. The one-electron transition $2a_{1g} \rightarrow 2e_{1g}$ results in excited states of $^1E_{1g}$ and $^3E_{1g}$ symmetries, whereas $1e_{2g} \rightarrow 2e_{1g}$ gives excited states of $^1E_{1g}$, $^3E_{1g}$, $^1E_{2g}$, and $^3E_{2g}$ symmetries. Theoretical expressions for the spin-allowed transitions, including configurational interaction between the two $^1E_{1g}$ states, were given in our recent communication.[28] These expressions, as well as those for the singlet–triplet transitions, are set out in Table I. All the expressions were derived by standard procedures[36] using a strong-field approach.

The ground electronic state of the ferricenium ion has been shown by esr[20,22] and magnetic susceptibility studies[35] to be $^2E_{2g}(1e_{2g})^3(2a_{1g})^2$. This state is split into two Kramers doublets by spin–orbit coupling (E'' and A', A'' in D_5'). Crystal fields of symmetry lower than D_5 mix E'' and A', A'' and affect the magnitude of the splitting. Similarly, the $^2E_{1g}$ and $^2E_{2g}$ excited states resulting from d–d transitions are each expected to split into two Kramers doublets. However, the splitting of the two Kramers doublets will be small relative to the transition energies and thus will not be included in our treatment of the d–d transitions in the ferricenium ion. Eight spin-allowed d–d transitions are predicted (spin-forbidden transitions will not be discussed) from three one-electron transitions: $^2E_{2g} \rightarrow {}^2A_{1g}$ for the $2a_{1g} \rightarrow 1e_{2g}$ one-electron transition; $^2E_{2g} \rightarrow {}^2E_{1g}$ and $^2E_{2g}$ for $2a_{1g} \rightarrow 2e_{1g}$; $^2E_{2g} \rightarrow 2\,{}^2E_{1g}$, $^2E_{2g}$, $^2A_{1g}$, and $^2A_{2g}$ for $1e_{2g} \rightarrow 2e_{1g}$. The theoretical transition-energy expressions are given in Table I. There is no configuration interaction between the two $^2A_{1g}$ states and likewise the ground-state $^2E_{2g}$ does not mix with the $^2E_{2g}$ excited states. In the theoretical expressions for the three $^2E_{1g}$ transitions configurational interaction was not included, but in the numerical treatment it was incorporated by matrix diagonalization using the following nonzero off-diagonal elements: $H_{ab} = 4\sqrt{3}B$, $H_{ac} = 2\sqrt{6}B$, and $H_{bc} = 3\sqrt{2}B$.

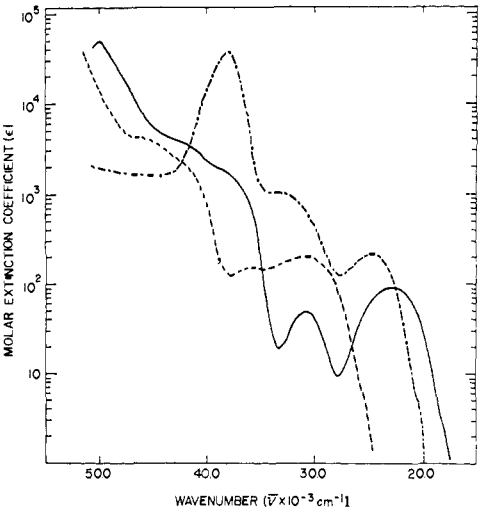

Figure 2. Electronic spectra of d^6 metallocenes in solution at 300°K: $Fe(cp)_2$ in isopentane (——), $Ru(cp)_2$ in isopentane (– – –), $[Co(cp)_2]ClO_4$ in aqueous solution (–·–·–).

Electronic Spectra of d^6 Metallocenes

The room-temperature absorption spectra of three d^6 metallocenes (ferrocene, ruthenocene, and cobalticenium) are displayed in Figure 2; band positions and intensities are given in Table II for these three complexes as well as for phenylferrocene. Similarities in band shapes and intensities are apparent in these spectra. We have elected to use ferrocene as the model molecule

(36) C. J. Ballhausen, "Introduction to Ligand Field Theory," McGraw-Hill, New York, N. Y., 1962.

Table II. The Ultraviolet and Visible Absorption Spectra of Four d^6 Metallocenes

Molecule	Band identification	Band, cm^{-1}	ϵ	$f \times 10^3$
$Fe(cp)_2$	I[a]	18,900	~7	
	II[a,b]	22,700 (21,800) (24,000)	9.10 (36) (72)	1.9 (0.3) (1.1)
	III[a]	30,800	49.0	0.75
	IV[c,d]	37,700	1,600	
	V[c,d]	41,700	3,500	
	VI[d]	50,000	51,000	730
$Ru(cp)_2$	I[a]	26,000	~5	
	II[a,b]	31,000 (29,500) (32,500)	200 (120) (160)	5.0 (1.5) (2.4)
	III[a]	36,600	150	
	IV[c,d]	42,000	2,000	
	V[c,d]	46,100	4,200	
	VI[d]	>51,300	>50,000	
$Co(cp)_2^+$	I[e]	21,800	~7	
	II[b,e]	24,600 (24,300) (26,400)	220 (140) (120)	3.8 (1.3) (1.5)
	III[e]	33,300	1,200	
	VI[e]	38,000	38,000	500
Fe(Ph-cp)(cp)	I[a]	~17,500	~5	
	II[a,b]	22,400 (20,800) (23,000)	310 (160) (320)	6.1 (1.3) (4.3)
	III[a]	29,500	850	
		31,400	1,250	
		36,100	10,100	
		42,000	16,300	
	VI[d]	>50,000	>30,000	

[a] Measured in EPA. [b] Band can be resolved into two submaxima at 77°K; Gaussian resolution gives the bands in parentheses. [c] Shoulder. [d] Measured in isopentane. [e] Measured as the perchlorate salt in aqueous solution.

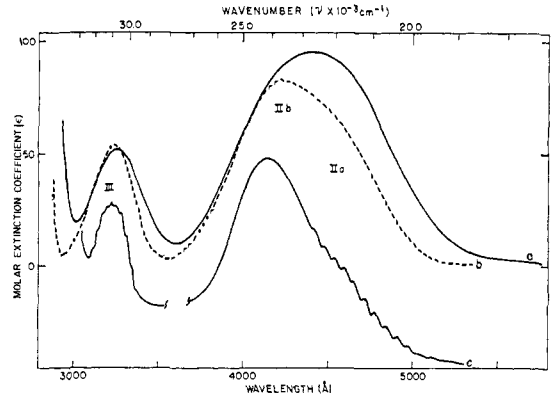

Figure 3. Visible absorption spectra of ferrocene at various temperatures: (a) EPA solution at 300°K, (b) EPA glass at 77°K, (c) single crystal at 4.2°K. The intensity of curve c is not to scale.

in the following discussion; absorption spectral data for the other ferrocene-like molecules will be discussed when providing insight or support for the ferrocene assignments. As a matter of convenience, the bands in the intensity range $10 < \epsilon \leq 1000$ will be considered first.

Spin-Allowed d–d Transitions. The d^6 metallocenes exhibit two low-intensity bands in the visible range (see Figure 2 and Table II). The two ferrocene bands at 22,700 and 30,800 cm^{-1} (*i.e.*, band systems II and III, respectively, in Figure 2) have generally been assigned as d–d transitions.[24,25,28] Using strong-field theory three spin-allowed d–d transitions (two $^1A_{1g} \rightarrow {}^1E_{1g}$ and one $^1A_{1g} \rightarrow {}^1E_{2g}$) are expected for ferrocene (see Theory section). There has been considerable controversy as to the location of these three transitions. Initial reports[23,37] of the resolution of band system II into two bands have not been accepted by other workers.

(37) L. D. Dave, D. F. Evans, and G. Wilkinson, private communication quoted in ref 24.

The ferrocene single-crystal low-temperature absorption spectra recently reported by Stephenson and Winterrowd[27] (at 77°K) and by Sohn, *et al.*[28] (at 4.2°K), have conclusively shown that the ferrocene 22,700-cm^{-1} system consists of two bands (see Figure 3). In this section we will expand on our ferrocene communication and generalize to other ferrocene-like molecules.

Band system II in the 4.2°K single-crystal ferrocene spectrum (see Figure 3) appears as a vibrationally structured band shouldering a more intense, unstructured band. Band system III also develops vibrational structure at liquid helium temperature. Details of peak position and spacing for the vibrational structure in these bands systems are given in Table III. Absorp-

Table III. Vibrational Structure of Ferrocene Bands IIa and III

System	$\bar{\nu}$, cm^{-1}	$\Delta\bar{\nu} = \bar{\nu}_n - \bar{\nu}_{n-1}$
IIa	19,870 ± 20	
	20,120 ± 10	250
	20,400 ± 10	280
	20,670 ± 10	270
	20,970 ± 10	300
	21,240 ± 10	270
	21,510 ± 10	270
	21,770 ± 10	260
	22,050 ± 10	280
	22,330 ± 10	280
	22,640 ± 20	310
III	29,590 ± 20	
	29,860 ± 20	270
	20,150 ± 20	290
	30,450 ± 20	300
	30,690 ± 20	240
	30,950 ± 20	260
	31,210 ± 20	260
	31,500 ± 20	290
	31,760 ± 20	260
	32,020 ± 20	260

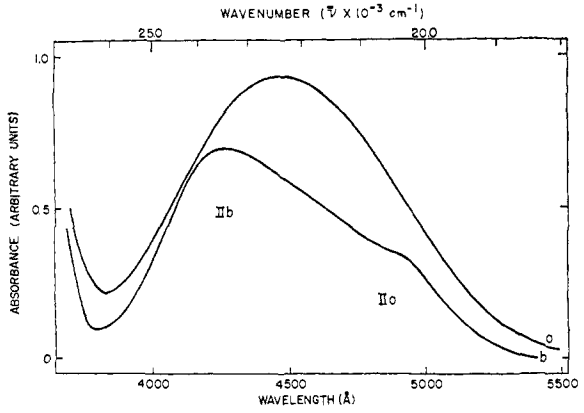

Figure 4. Visible absorption spectra of phenylferrocene: (a) EPA solution at 300°K, (b) single crystal at 4.2°K.

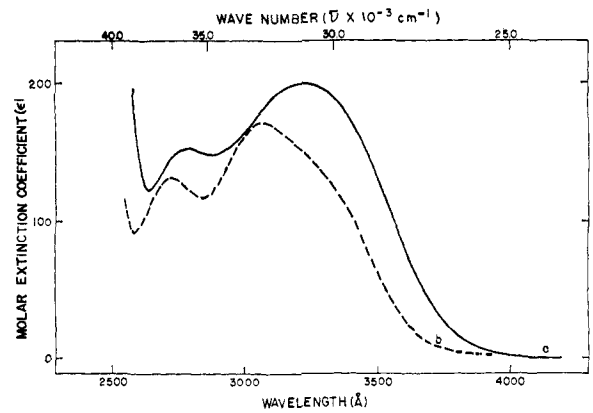

Figure 5. Near-ultraviolet absorption spectra of ruthenocene: (a) EPA solution at 300°K, (b) EPA glass at 77°K.

tion spectra at 4.2°K were also obtained for thick single crystals of ferrocene to ensure that we had detected all the vibrational bands in the structure. The spacing of the vibrational structure in each band is 240–300 cm^{-1}, which is the excited-state totally symmetric ring–metal vibration (a_{1g}; the ground-state value is 309 cm^{-1}).[38] The nonuniformity in spacing in each system is seemingly outside of the experimental uncertainty in peak location and is possibly attributable to having more than one vibronic origin.

We have been able to resolve into two bands the low-energy band system (corresponding to system II of ferrocene) in both phenylferrocene and ruthenocene. In Figure 4 the temperature dependence of band system II of phenylferrocene is depicted. The 77°K spectrum of phenylferrocene is not shown in Figure 4 but could be obtained using either an EPA glass or a single crystal. The single-crystal spectrum of phenylferrocene at 4.2°K shows no vibrational structure, but in this case it is more apparent that band system II is composed of two transitions. Similar comments can be made concerning band system II in ruthenocene. The 77°K absorption spectrum of ruthenocene in EPA glass, as reproduced in Figure 5, shows clearly two peaks in band system II. The probability of an impurity as the explanation for the shoulder in ferrocene has been eliminated. In the cobalticenium ion, the resolution of bands IIa and IIb is poor; nevertheless, the asymmetric band at 77°K could be resolved into two Gaussian curves.

The three expected d–d transitions have thus been located in these d^6 metallocenes. Franck–Condon maxima were obtained in each case by Gaussian analysis of the 77°K spectra (plotted in units of ϵ *vs.* frequency) and were used as transition energies. The three observed d–d bands are assigned in Table IV to the three spin-allowed d–d transitions. This assignment scheme for the three bands is unique in the sense that it is the only one which yields a physically realistic value for the Racah parameter B. The proposed interpretation is also consistent with the observed temperature behavior of these bands. Band IIa decreases more in intensity than bands IIb and III when the temperature is lowered (see Figure 3). In agreement with this observation our assignment has attributed more d–d character to band IIa than the other two bands (*i.e.*, band IIa results from the one-electron transition $2a_{1g} \rightarrow 2e_{1g}$). The ligand-field parameters B, $\Delta_1 = \epsilon^c(e_{2g} - 2a_{1g})$, and $\Delta_2 = \epsilon^c(2e_{1g} - 2a_{1g})$ have been evaluated for the four d^6 metallocene complexes and are given in Table IV. It seems worthwhile to point out that the parameters B and Δ_1 were evaluated without any assumptions from appropriate combinations of the three equations. In order to evaluate Δ_2 it is necessary to assume a value for the ratio C/B. We have taken $C/B = 4.0$, which is generally reasonable for the case of transition metal complexes. The Δ_2 values thus obtained are only slightly affected by changing the C/B ratio, since the value of B is small in these metallocenes.

Table IV. Spin-Allowed Ligand-Field Absorption Transitions and Parameters for d^6 Metallocenes[a]

	$Fe(cp)_2$	$Ru(cp)_2$	$Co(cp)_2^+$	Fe(Ph–cp)-(cp)
$^1A_{1g} \rightarrow a^1E_{1g}$	21,800	29,500	24,300	20,800
$^1A_{1g} \rightarrow {}^1E_{2g}$	24,000	32,500	26,400	23,000
$^1A_{1g} \rightarrow b^1E_{1g}$	30,800	36,600	33,300	29,500
Δ_2	22,000	29,800	24,400	21,000
Δ_1	−7,100	−6,600	−7,200	−6,900
B	390	260	400	370
β	0.42	0.42	0.36	0.40

[a] Energies in reciprocal centimeters.

The values of the ligand-field parameters for the d^6 metallocenes are of some interest. The three transitions move to higher energy in the series Fe < Co < Ru, reflecting the increasing ligand-field splitting. Thus Δ_2 increases parallel to the probable increase in ring → metal bonding, Fe < Co < Ru. The relatively small Racah electron-repulsion parameters B in these d^6 metallocenes indicate appreciable covalency. The B value for ferrocene (390 cm^{-1}) compares closely with that for $Fe(CN)_6^{4-}$ (380 cm^{-1}).[39] Finally, it can be seen in Table IV that in every case the one-electron energy of the a_{1g} orbital is higher than that of the e_{2g} level. This is in agreement with qualitative molecular orbital theory, because the filled, primarily metal e_{2g} level is expected to derive some stabilization from $d\pi \rightarrow$ ring bonding with the unfilled ligand level of e_{2g} symmetry.

The ligand-field parameters are also useful in predicting the location of the spin-forbidden absorption transitions, a subject to which we now turn.

Spin-Forbidden d–d Transitions. Three very weak spin-forbidden absorption bands (spin-forbidden d–d

(38) J. Bodenheimer, E. Loewenthal, and W. Low, *Chem. Phys. Lett.*, 3, 715 (1969).

(39) J. J. Alexander and H. B. Gray, *J. Amer. Chem. Soc.*, 90, 4260 (1968).

Table V. Spin-Forbidden d–d Transitions for d^6 Metallocenes[a]

	$Fe(cp)_2$	$Ru(cp)_2$	$Co(cp)_2^+$	Fe(Ph–cp)(cp)
$^1A_{1g} \rightarrow b^3E_{1g}$	22.4	30.9	24.8	21.5
$^1A_{1g} \rightarrow {}^3E_{2g}$	20.9	30.3	23.2	20.1
$^1A_{1g} \rightarrow a^3E_{1g}$	18.6 (18.9)[b]	27.3 (26.0)[b]	20.8 (21.8)[b]	17.7 (17.5)[b]

[a] Transition energies ($\bar{\nu} \times 10^{-3}$, cm^{-1}) were calculated using the ligand-field parameters resultant from the analysis of the spin-allowed d–d bands. [b] Experimentally observed in absorption in this work.

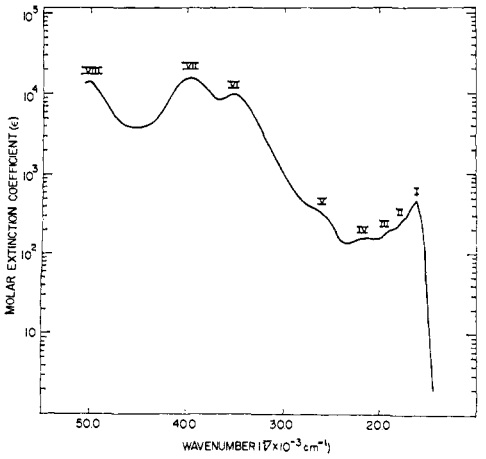

Figure 6. Electronic absorption spectrum of ferricenium ion in 0.01 M $HClO_4$ aqueous solution at 300°K.

bands) of ferrocene were reported by Scott and Becker.[24] Of these, the existence of the first two ($\epsilon < 1$), which could only be produced by gaussian analysis, is doubtful. A careful absorption measurement below 4000 Å on ruthenocene failed to detect any bands corresponding to these alleged ferrocene bands. Band I ($\epsilon \sim 7$) of ferrocene, on the other hand, has been characterized by iodine perturbation experiments.[24,40] This band system has been observed in all four d^6 metallocenes under investigation here. Therefore, we conclude that band I is the only singlet–triplet transition which can be observed in the absorption spectra of these molecules.

The positions of the three spin-forbidden d–d transitions were calculated using the expressions in Table I and the values of Δ_1, Δ_2, and B which were evaluated in the previous section. As shown in Table V, the predicted energy of the lowest singlet–triplet transition in each of the d^6 metallocenes is in good agreement with the observed absorption position of band I.

Charge-Transfer Bands. In the ultraviolet region of the ferrocene solution absorption spectrum (see Figure 2) a strong band (ϵ 51,000) at 50,000 cm^{-1} (band VI) and two shoulders at 37,700 and 41,700 cm^{-1} (bands IV and V) have been observed as reported.[24,25] In Figure 2 and Table II it can be seen that ruthenocene exhibits a similar ultraviolet absorption spectrum, with the three bands slightly blue shifted. However, in the isoelectronic cobalticenium ion only a single strong band appears at 38,000 cm^{-1}, with no apparent shoulders. Band VI (ϵ 38,000) of the cobalticenium ion has an oscillator strength similar to that of band VI of ferrocene and ruthenocene and most probably is due to the same type of fully allowed charge-transfer transition. Two different types of charge transfer occur in metal complexes. For instance, in the d^6 hexacyanometalate complexes $Fe(CN)_6^{4-}$ and $Co(CN)_6^{3-}$ M → L charge-transfer bands have been observed[39,41] and the charge-transfer transition energy increases on increasing the positive charge of the central metal ion. On the other hand, L → M charge-transfer bands have been observed in d^6 hexahalometalate systems.[42] Here the transition energy decreases markedly with increasing positive charge of the metal atom. The energy of band VI in the d^6 metallocenes is in the order $Co(cp)_2^+ < Fe(cp)_2 < Ru(cp)_2$, which is the order of decreasing metal electronegativity. Thus we conclude that band VI is a L → M charge transfer.

In terms of the energy level scheme in Figure 1 there is only one possible L → M assignment for band VI, $1e_{1u} \rightarrow 2e_{1g}$, since the $1a_{2u}$ level is estimated to be too far from the $2e_{1g}$ level. The one-electron transition $1e_{1u} \rightarrow 2e_{1g}$ results in three singlet excited states, $^1A_{1u}$, $^1A_{2u}$, and $^1E_{2u}$, but only the transition to the $^1A_{2u}$ state is allowed. Therefore, band system VI in the d^6 metallocenes is assigned as a $^1A_{1g} \rightarrow {}^1A_{2u}$ ($1e_{1u} \rightarrow 2e_{1g}$) transition.

The characterization of the two shoulders, systems IV and V, is not as definitive, since the band positions and intensities are both difficult to determine accurately and the reported[24,43,44] substitutional effects are doubtful. For instance, in phenylferrocene, one shoulder and three strong bands have been observed (see Table II), but the two bands at 36,100 and 42,000 cm^{-1} are probably due to the primarily phenyl group transitions $^1A_{1g} \rightarrow {}^1B_{2u}$ (39,400 cm^{-1}) and $^1A_{1g} \rightarrow {}^1B_{1u}$ (49,000 cm^{-1}). These two bands[45,46] are quite variable, both in band position and intensity, when benzene is substituted.

Electronic Spectra of d^5 Metallocenes

An aqueous solution of ferricenium ion, $Fe(cp)_2^+$, exhibits at room temperature four bands and at least four shoulders, as can be seen in Table VI and Figure 6.

Table VI. Electronic Absorption Spectrum of Aqueous $Fe(cp)_2^+$ [a]

	$\bar{\nu}$, cm^{-1}	ϵ	$f \times 10^3$
I	16,200	450	2.3
II[b]	17,700	250	
III[b]	19,100	190	
IV[b]	21,400	150	
V[b]	26,300	350	
VI	35,300	9,700	~120
VII	39,900	16,000	162
VIII	50,500	14,000	

[a] 10 M LiCl aqueous solution. [b] Shoulder.

(40) A. N. Nesmeyanov, E. G. Perevalova, and O. A. Nesmeyanova, *Dokl. Akad. Nauk SSSR*, **100**, 1099 (1955).

(41) H. B. Gray and N. A. Beach, *J. Amer. Chem. Soc.*, **85**, 2922 (1963).

(42) C. K. Jorgensen, *Mol. Phys.*, **2**, 309 (1959).

(43) V. Weinmayr, *J. Amer. Chem. Soc.*, 77, 3012 (1955).

(44) K. I. Grandberg, S. P. Gubin, and E. G. Perevalova, *Izv. Akad. Nauk SSSR, Ser. Khim.*, 549 (1966).

(45) H. H. Jaffe and M. Orchin, "Theory and Application of Ultraviolet Spectroscopy," Wiley, New York, N. Y., 1962.

(46) A. R. Gillam and E. S. Stern, "Electronic Absorption Spectroscopy," Arnold, London, 1958.

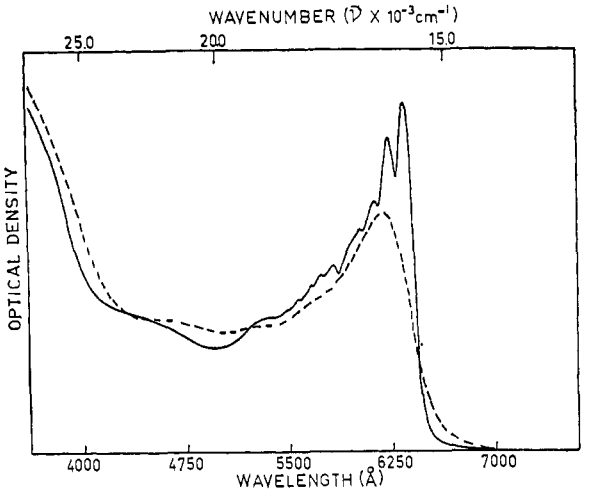

Figure 7. Visible absorption spectra of $[Fe(cp)_2]$ (BF_4) in 10 *M* LiCl aqueous solution: (- - -) 300°K, (——) 77°K.

The ground electronic state $(1e_{2g})^3(2a_{1g})^2$ of the ferricenium ion has been investigated by various techniques.[20,21,35] In this section we will show how absorption spectroscopy applied to various ferricenium compounds will give information as to the location and character of various excited states. In some instances this information about excited states will be shown to give insight into the ferricenium ion ground electronic state. In particular, ferricenium band I is a new feature, not observable in ferrocene, which will be valuable in the characterization of electronic structure.

Band System I. This ferricenium band system has moderate intensity and exhibits vibrational structure at 77°K in a LiCl glass (see Figure 7). In our communication[21] the observed vibrational progression was assigned to the symmetric ring–metal stretching frequency (the corresponding ground-state ferrocene a_{1g} frequency is 309 cm^{-1}). Details of the peak positions in this 77°K LiCl glass spectrum are given in Table VII. It can be seen that the vibrational spacings in the band system are approximately the same, but on the higher energy side irregular intensities complicate matters. The oscillator strength of band I increases approximately 20% in going from 300 to 77°K (2.3×10^{-3}–2.7×10^{-3}). This type of temperature dependence rules against a d–d transition. We have assigned this band as the ligand-to-metal charge transfer $^2E_{2g} \rightarrow {}^2E_{1u}$.[21] The above evidence as well as an analogy with ferricyanide were the reasons for our assignment of the ferricenium band I to the transition of an electron from the bonding ring level $1e_{1u}$ to the hole in the essentially nonbonding metal $1e_{2g}$ orbital (see Figure 1). Prins has shown[47] that band I shifts significantly upon ring substitution and on this basis independently assigned it to the $^2E_{2g} \rightarrow {}^2E_{1u}$ transition. Our studies of the substitutional behavior of band I are in accord with those of Prins. Two substituted ferricenium salts were prepared: $[Fe(n\text{-Bu-cp})(cp)]PF_6$ and $[Fe(n\text{-Bu-cp})_2]PF_6$. It was found convenient to perform the absorption spectroscopic studies of these two salts and $[Fe(cp)_2]PF_6$ in KBr pellets. The results of these studies can be seen in Figures 8–10. The 16,200-cm^{-1} band system of $[Fe(cp)_2]PF_6$ in a KBr pellet undergoes a red shift upon ring substitution, a result that is apparent from either a comparison of the room-temperature or 77°K absorption spectra. Thus this band system appears at 16,000 cm^{-1} for $[Fe(n\text{-Bu-cp})(cp)]PF_6$ and shows a drastic shift to 14,800 cm^{-1} for $[Fe(n\text{-Bu-cp})_2]PF_6$ at room temperature. The apparent origins (0,0) in the progressions at 77°K for the monobutylated and dibutylated

Table VII. Vibrational Structure of Band I of $Fe(cp)_2^+$ in Solution[a]

$\bar{\nu}$, cm^{-1}	$\Delta\bar{\nu} = \bar{\nu}_n - \bar{\nu}_{n-1}$	Assignment
15,730 ± 10		(0,0)
16,020 ± 10	290	(1,0)
16,290 ± 10	270	(2,0)
16,590 ± 10	300	(3,0)
16,860 ± 10[b]	270	
17,150 ± 10	290	
17,420 ± 10	270	
17,700 ± 20	280	
17,950 ± 20	250	
18,240 ± 20	290	
18,550 ± 20	310	
18,800 ± 20	250	

[a] 10 *M* LiCl aqueous solution at 77°K. [b] This component is not clearly resolved from the 16,590-cm^{-1} band.

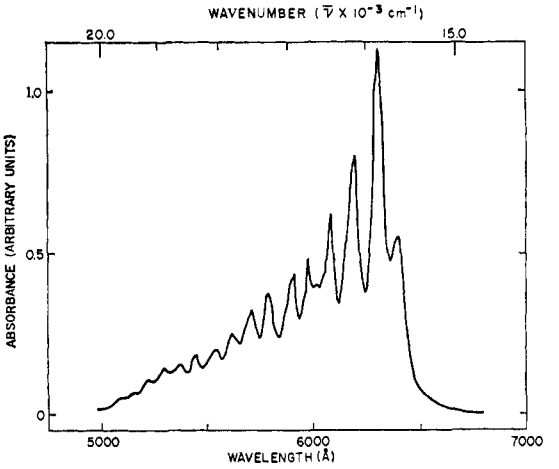

Figure 8. Vibrational structure of band I for a KBr pellet of $[Fe(cp)_2]PF_6$ at 77°K.

Table VIII. Vibrational Structure of Band I of $[Fe(cp)_2](CCl_3CO_2H)_3$[a]

$\bar{\nu}$, cm^{-1}	$\Delta\bar{\nu} = \bar{\nu}_n - \bar{\nu}_{n-1}$	$\Delta\bar{\nu}' = \bar{\nu}_{n'} - \bar{\nu}_{n'-1}$	Assignment
			$A_{1g}(W_4)$
15,640 ± 10			(0,0)
15,800 ± 10			(0,0)′
15,940 ± 10	300		(1,0)
16,100 ± 10		300	(1,0)′
16,270 ± 10	330		(2,0)
16,410 ± 10		310	(2,0)′
16,580 ± 10	310		(3,0)
16,710 ± 10		300	(3,0)′
16,880 ± 10	300		(4,0)
17,020 ± 20		310	(4,0)′
17,190 ± 20	310		(5,0)
17,320 ± 20		300	(5,0)′
b			

[a] KBr pellet spectrum at 77°K. [b] The progression continues down to ~5100 Å but the structure is poorly resolved.

(47) R. Prins, *Chem. Commun.*, 280 (1970).

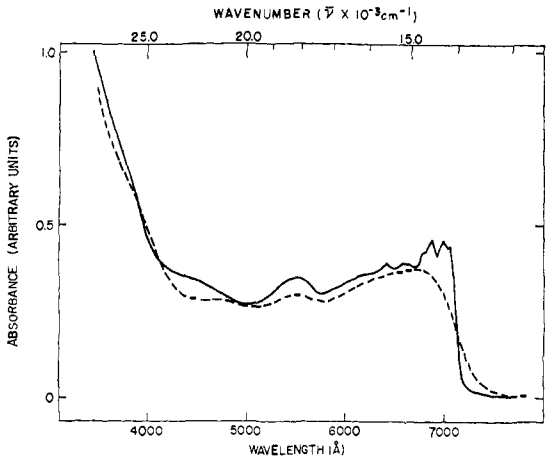

Figure 9. Visible absorption spectra of [Fe(*n*-Bu-cp)(cp)][PF_6] in KBr pellet: (- - -) 300°K, (——) 77°K.

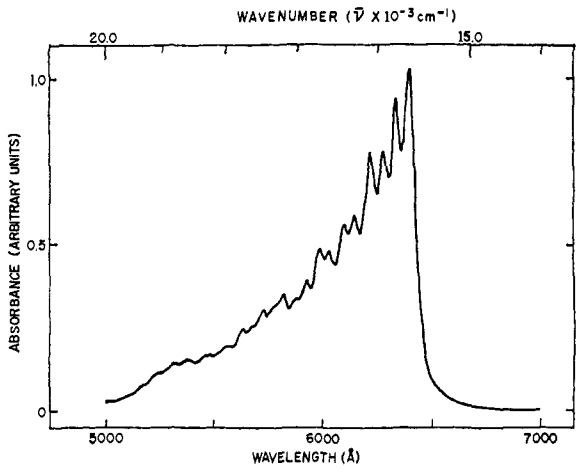

Figure 11. Vibrational structure of band I for a KBr pellet of [$Fe(cp)_2$][CCl_3CO_2H]$_3$ at 77°K.

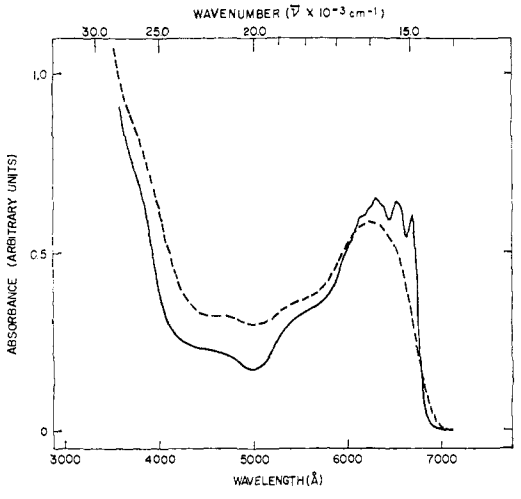

Figure 10. Visible absorption spectra of [Fe(*n*-Bu-cp)$_2$][PF_6] in KBr pellet: (- - -) 300°K; (——) 77°K.

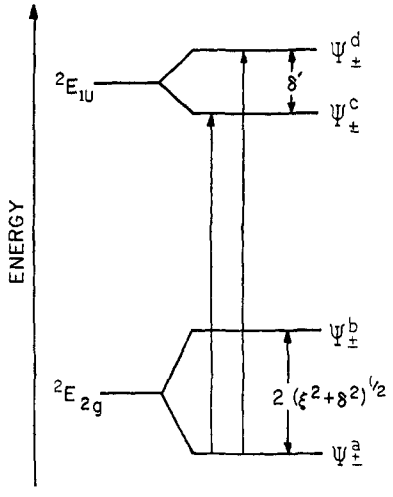

Figure 12. Energy level scheme for the $^2E_{2g}$ ground and $^2E_{1u}$ excited states of ferricenium ion with inclusion of spin-orbit coupling and low-symmetry crystal-field components.

ferricenium hexafluorophosphates appear at 14,950 and 14,160 cm^{-1}, respectively, compared to 15,630 cm^{-1} for [$Fe(cp)_2$]PF_6.

As can be seen in Figure 8, band system I of the ferricenium ion shows markedly better resolution of vibrational structure when the compound is pelleted in KBr than we had obtained for a LiCl glass. In fact, in appearance each peak in the LiCl glass spectrum seems to be split into two. This doubling of peaks can be best seen in the 77°K spectrum of [$Fe(cp)_2$][CCl_3CO_2H]$_3$, depicted in Figure 11. It seems worthwhile, at this time, to point out that [$Fe(cp)_2$]BF_4 gives the same 77°K absorption spectrum in either a KBr pellet or in a LiCl glass. We will return to this point later in the discussion.

Before we begin to develop a detailed assignment of the vibrational structure in these ferricenium spectra, it is helpful to review what is known about the ground state of the ferricenium ion. Such a review will aid our speculation as to the expected appearance of the ferricenium $^2E_{2g} \rightarrow {}^2E_{1u}$ transition under moderate resolution. As discussed in the Theory section, the $^2E_{2g}$-$(a_{1g})^2(e_{2g})^3$ ground electronic state of the ferricenium ion is split into E'' and A', A'' Kramers doublets by spin-orbit coupling. The E'' and A', A'' levels are mixed by crystal fields of symmetry lower than D_5 into the Kramers doublets labeled $\psi_\pm{}^a$ and $\psi_\pm{}^b$ in the schematic energy diagram shown in Figure 12. We propose that the $^2E_{1u}$ excited state is also split, principally by components of the low-symmetry crystal field. The resulting Kramers doublets, denoted $\psi_\pm{}^c$ and $\psi_\pm{}^d$ in Figure 12, are mixtures of the D_5' levels E' and E''. Since both $\psi_\pm{}^a(^2E_{2g}) \rightarrow \psi_\pm{}^c(^2E_{1u})$ and $\psi_\pm{}^a(^2E_{2g}) \rightarrow \psi_\pm{}^d(^2E_{1u})$ are allowed transitions, a doubled vibrational progression could result from a progression of the totally symmetric vibration on each origin. The splitting of the excited state $^2E_{1u}$ would be due essentially to a distortion which influences the energy of the carbon p orbitals, $\delta' = \langle e_{1u}{}^+|H_{\text{eff}}'|e_{1u}{}^-\rangle$.

The vibrational structure which appears in the 77°K spectrum of [$Fe(cp)_2$] [CCl_3CO_2H]$_3$ is the easiest to explain. As noted previously, band system I in this spectrum is most likely a progression of doublets resulting from a splitting of the excited state ($^2E_{1u} \rightarrow \psi_\pm{}^c$ and $\psi_\pm{}^d$). The first two peaks, 15,640 and 15,800 cm^{-1}, are probably the origins (0,0) of the $\psi_\pm{}^a \rightarrow \psi_\pm{}^c$ and $\psi_\pm{}^a \rightarrow \psi_\pm{}^d$ transitions. The distortion parameter of the $^2E_{1u}$ excited state, δ', may be estimated as 140 cm^{-1} (average of the spacings of the doublets) for [$Fe(cp)_2$][CCl_3CO_2H]$_3$. The details of our tentative as-

signment are given in Table VIII. The 77°K single-crystal spectrum of $[Fe(cp)_2](CCl_3CO_2H)_3$ shows essentially the same vibrational structure for band system I. In addition, at higher energy two new bands (20,600 and 22,400 cm^{-1}) appear which were either not present in the KBr pellet or solution spectra or have gained appreciable intensity. The intensity of these two bands is slightly in excess of that of band system I. One possible explanation is that these two bands in the single-crystal spectrum are intermolecular charge-transfer bands.

In the case of $[Fe(cp)_2]PF_6$ each vibrational component (see Figure 8) in the 77°K KBr pellet spectrum is not symmetric (some appear to be shouldered). The two electronic origins are not easy to locate in this case. However, we have made a tentative assignment (see Table IX) analogous to that proposed for band system I of $[Fe(cp)_2](CCl_3CO_2H)_3$. If the first two components at 15,630 and 15,850 cm^{-1} are taken as the two origins, the distortion in the excited state, δ', is estimated as 200 cm^{-1}. It seems that the first progression with an origin at 15,630 cm^{-1} has a lower intensity than the second progression and probably causes shoulders on each of the components of the second progression. Further study of this band system I at 4.2°K may be helpful in better understanding the vibrational structure.

Table IX. Vibrational Structure of Band I of $[Fe(cp_2)]PF_6$[a]

$\tilde{\nu}$, cm^{-1} [c]	$\Delta\tilde{\nu} = \tilde{\nu}_n - \tilde{\nu}_{n-1}$	$\Delta\tilde{\nu} = \tilde{\nu}_{n'} - \tilde{\nu}_{n'-1}$	Assignment
15,630 ± 10			(0,0)
15,850 ± 10			(0,0)′
(15,930)	(300)		(1,0)
16,150 ± 10		300	(1,0)′
(16,230)	(300)		(2,0)
16,440 ± 10		290	(2,0)′
(16,530)	(300)		(3,0)
16,730 ± 10		290	(3,0)′
16,810[b]			
16,920			
17,010[b]			
17,220[b]			
17,290			
17,520			
17,580[b]			
17,810			
18,050			
18,130[b]			
18,370			
18,600			
18,690[b]			
18,910			
19,140			
19,420			
19,690			

[a] KBr pellet spectrum at 77°K; the frequencies in parentheses were calculated assuming an a_{1g} progression on the (0,0) origin. [b] Shoulder. [c] Uncertainties in peak positions are ±20 cm^{-1} unless otherwise specified.

It is clear from the above two cases that we are in fact dealing with a split excited state. In each substituted ferricenium ion salt the low-temperature spectrum also has the appearance of a doubled progression (see Figures 9 and 10). Band system I in the ferricenium spectrum is a reasonably sensitive function of the counterion as well as ring substitution. Similar results were found in the magnetic susceptibility studies,[35] where the distortion in the ferricenium $^2E_{2g}$ ground state (*i.e.*, $\delta = \langle e_{2g}^+|H_{eff}'|e_{2g}^-\rangle$) was found to be sensitive to counterion interchange as well as ring substitution.

Finally, we return to the LiCl glass spectrum and indulge in a brief discussion. The 77°K LiCl glass spectrum of the ferricenium ion and the 77°K KBr pellet spectrum of $[Fe(cp)_2]BF_4$ exhibit far less vibrational structure than the other cases; peaks are broader also. Two explanations come to mind: (a) there is an averaging of several environments and lower resolution ensues or (b) the distortion δ' approaches equality with the vibrational frequency causing excessive overlapping. Explanation a seems viable for the LiCl glass case, but is difficult to accept for the KBr spectrum of $[Fe(cp)_2]BF_4$. Magnetic susceptibility measurements have indicated[21,35] that the ground-state distortion experienced by the ferricenium ion in an aqueous solution is comparable to that felt by the ion in the tetrafluoroborate salt. Thus until further study, explanation b is the more attractive of the two.

Spin-Allowed d–d Transitions. In the visible region of the ferricenium ion spectrum four shoulders at 17,700, 19,100, 21,400 and 26,300 cm^{-1} (bands II–V) have been observed. These weak peaks appear at the same positions in all of the ferricenium salts, both in solutions and in KBr pellets. Their intensities and positions are nearly insensitive to ring substitution. Therefore, these shoulders may be assigned as essentially metal d–d transitions.

Theoretically, seven different spin-allowed d–d transitions are predicted for the ferricenium ion in the visible and uv region (see Theory section), excluding the lowest $^2A_{1g}$ transition, which is expected[21] to be in the ir range. Since we have fewer observed bands, the approach that we have taken is to calculate theoretical transition energies for different values of the three ligand field parameters, B, Δ_1, and Δ_2. Computer diagonalization was employed to account for configurational interaction in the case of the $^2E_{1g}$ transitions. Using the ferrocene parameters as guides, the ranges of the parameters investigated were: $-2000 > \Delta_1 > -14{,}000$ cm^{-1}; $22{,}000 < \Delta_2 < 35{,}000$ cm^{-1}; $400 < B < 700$ cm^{-1}. We found that the transition energies are in the order (giving only the symbol for the excited state) $a^2A_{1g} \ll a^2E_{1g} < a^2E_{2g} < b^2E_{1g} \sim b^2A_{1g} \sim {}^2A_{2g} < c^2E_{1g} \sim b^2E_{2g}$. Calculated ferricenium transition energies are given in Table X for the case where the parameters (B, Δ_1, Δ_2) are assumed to be the same as in ferrocene. Results are also tabulated for the calculation where Δ_1 and Δ_2 were taken from ferrocene but B was increased to 700 cm^{-1}.

Table X. Ligand-Field Bands of $Fe(cp)_2^+$

Transitions	Calcd energy I[a]	Calcd energy II[b]	Exptl[c]
$^2E_{2g} \rightarrow a^2E_{1g}$	20,000	14,700	17,700
$\rightarrow a^2E_{2g}$	22,100	21,000	19,100
$\rightarrow b^2E_{1g}$	25,000	23,900	21,400
$\rightarrow b^2A_{1g}$	26,400	24,200	26,300
$\rightarrow {}^2A_{2g}$	26,400	24,200	
$\rightarrow c^2E_{1g}$	28,600	29,800	
$\rightarrow b^2E_{2g}$	29,800	31,600	

[a] $\Delta_1 = -7100$ cm^{-1}, $\Delta_2 = 22{,}000$ cm^{-1}, and $B = 390$ cm^{-1}. [b] $\Delta_1 = -7100$ cm^{-1}, $\Delta_2 = 22{,}000$ cm^{-1}, and $B = 700$ cm^{-1}. [c] Ordered in increasing energy.

Table XI. Selected Charge-Transfer Transitions of d^5 and d^6 Metallocenes

One-electron transitions	$Fe(cp)_2$ b	$Fe(cp)_2$ Excited states[a]	$Fe(cp)_2^+$ b	$Fe(cp)_2^+$ Excited states[a]
$2a_{1g} \rightarrow e_{2u}$	F	$(^1E_{2u})$	A	$^2E_{1u} + (^2A_{1u}) + (^2A_{2u})$
$1e_{2g} \rightarrow e_{2u}$	A	$^1E_{1u} + {}^1A_{2u} + (^1A_{1u})$	A	$3\,^2E_{2u} + {}^2E_{1u}$
$1e_{1u} \rightarrow 1e_{2g}$			A	$^2E_{1u}$
$1e_{1u} \rightarrow 2e_{1g}$	A	$^1A_{2u} + (^1A_{1u}) + (^1E_{2u})$	A	$2\,^2E_{2u} + {}^2E_{1u} + (^2A_{1u}) + (^2A_{2u})$
$1a_{2u} \rightarrow 1e_{2g}$			F	$(^2A_{2u})$

[a] Transitions to the excited states in parentheses are orbitally forbidden. [b] Allowed (A) or forbidden (F).

Table XII. Charge-Transfer Bands of Substituted and Unsubstituted Ferricenium Ions[a]

Band	$Fe(cp)_2^+$ $\bar{\nu}$, cm^{-1}	ϵ	$Fe(n\text{-Bu-cp})(cp)^+$ $\bar{\nu}$, cm^{-1}	ϵ	$Fe(n\text{-Bu-cp})_2^+$ $\bar{\nu}$, cm^{-1}	ϵ
I	16,190	450	16,000	330	15,390	340
VI[b]	35,310	9,700	34,770	8,600	34,360	9,400
VII	39,900	15,900	39,310	13,600	38,610	13,300
VIII	50,450	14,200	50,000	12,300	49,630	12,000
ϵ(VII)/ϵ(VIII)	1.11		1.10		1.11	

[a] 0.01 *M* $HClO_4$ aqueous solution. [b] Appears as a shoulder in substituted ferricenium ions.

This latter treatment is based on the assumption that the parameter change in going from $Fe(cp)_2$ to $Fe(cp)_2^+$ is analogous to changes observed[39] in going from $Fe(CN)_6^{4-}$ to $Fe(CN)_6^{3-}$. Although neither calculation gives particularly good agreement with the experimental peak positions, the assignments for the first three ligand-field bands are reasonably satisfactory.

Further work is needed to better resolve these weak peaks. Perhaps the ferricenium ion should be substituted such that band system I moves to much lower energy. This would make possible an improved definition in peak position for the lower energy d–d bands.

Charge-Transfer Bands. The solution spectrum of the ferricenium ion shows three bands at 35,300, 39,900, and 50,500 cm^{-1} (bands VI–VIII) in the ultraviolet region (see Figure 6). These three bands have large oscillator strengths ($f > 0.1$) and as such they result from allowed transitions. In comparison with band VI of ferrocene ($f \sim 0.7$), the ferricenium band VIII has a somewhat lower oscillator strength. However, it is probable that band VIII arises from a $1e_{1u} \rightarrow 2e_{1g}$ transition. The band systems VI and VII of the ferricenium ion, which appear in the region of the ferrocene shoulders IV and V, may be regarded as allowed charge-transfer transitions which are either forbidden or do not occur in the ferrocene molecule.

Bands VI and VII may be assigned after consideration of the allowed charge-transfer transitions. By group theory we know that to be allowed a transition from the $^2E_{2g}$ ground state must be to an excited state of $^2E_{1u}$ or $^2E_{2u}$ symmetry. We have summarized in Table XI the energetically feasible charge-transfer transitions (see the MO diagram, Figure 1) which give $^2E_{1u}$ or $^2E_{2u}$ excited states.

We have already assigned the low-energy charge-transfer band at 16,200 cm^{-1} in $Fe(cp)_2^+$ as the allowed transition from the $1e_{1u}$ level to the hole in the $1e_{2g}$ level (see Figure 12). Bands VI and VII of the ferricenium ion could be envisioned as transitions from some other low-lying bonding levels to the same hole in the essentially metal e_{2g} orbital. However, no such transitions are electric dipole allowed. Two types of transitions remain as candidates: metal-to-ligand transitions from the two essentially nonbonding orbitals $2a_{1g}$ and $1e_{2g}$ to e_{2u} and the ligand-to-metal charge-transfer transitions from $1e_{1u}$ to $2e_{1g}$.

Since the metal-to-ligand transitions to e_{2u} are allowed but not observed in the case of ferrocene, we much prefer the ligand-to-metal charge-transfer assignment for bands VI and VII of the ferricenium ion. It is our contention that band VI in the ferrocene spectrum results from the $1e_{1u} \rightarrow 2e_{1g}$ transition and that this same band is present in the ferricenium spectrum. The $1e_{1u} \rightarrow 2e_{1g}$ transition results in only one allowed excited state ($^1A_{2u}$) in ferrocene, but gives three allowed states ($^2E_{1u}$ and two $^2E_{2u}$) in the ferricenium case. Therefore, the three strong bands (VI, VII, and VIII) in the ferricenium spectrum are nicely accounted for by the single one-electron transition $1e_{1u} \rightarrow 2e_{1g}$. Strong evidence in support of this assignment is found in the observation that all of the three bands show red shifts upon ring substitution (see Table XII) by an energy comparable to the observed shifts of band system I of the ferricenium ion. This latter band system is definitely a ligand-to-metal charge-transfer transition. Finally, we note that the ratio of the intensities of the two highest energy ferricenium bands ($\epsilon_{VII}/\epsilon_{VIII}$) is almost constant among the unsubstituted and substituted ferricenium ions.

Acknowledgments. This research was supported by the National Science Foundation. We thank Professor C. J. Ballhausen for several stimulating discussions.